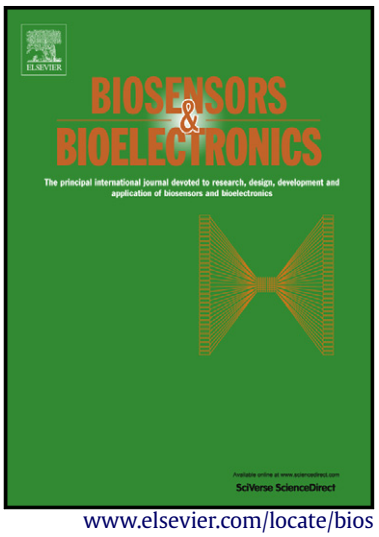


www.elsevier.com/locate/bios

# Self-Assemble $ZnMn_2O_4$ Hierarchical Hollow Microspheres into Self-Supporting Architecture for Enhanced Biosensing Performance

Minggang Zhao, Bin Cai, Ye Ma, Hi Cai, Jingyun Huang, Xinhua Pan, Haiping He, Zhizhen Ye

PII: S0956-5663(14)00392-3
DOI: http://dx.doi.org/10.1016/j.bios.2014.05.051
Reference: BIOS6813

To appear in: *Biosensors and Bioelectronics*

Received date: 6 May 2014
Accepted date: 18 May 2014

Cite this article as: Minggang Zhao, Bin Cai, Ye Ma, Hi Cai, Jingyun Huang, Xinhua Pan, Haiping He, Zhizhen Ye, Self-Assemble $ZnMn_2O_4$ Hierarchical Hollow Microspheres into Self-Supporting Architecture for Enhanced Biosensing Performance, *Biosensors and Bioelectronics,* http://dx.doi.org/10.1016/j.bios.2014.05.051

# Self-Assemble $ZnMn_2O_4$ Hierarchical Hollow Microspheres into Self-Supporting Architecture for Enhanced Biosensing Performance

Minggang Zhao[1], Bin Cai[1], Ye Ma[1], Hi Cai[1], Jingyun Huang[1,2], Xinhua Pan[1], Haiping He[1], Zhizhen Ye[1,2]*

[1]Department of Materials Science and Engineering, State Key Laboratory of Silicon Materials, Zhejiang University, Hangzhou 310027, China

[2] Cyrus Tang Center for Sensor Materials and Applications, Zhejiang University

## Abstract

We demonstrate a facile and scalable approach to fabricate and self-assemble the hierarchical hollow microspheres into self-supporting architecture by naturally grown branches. The supporting branches can afford integrated transport channels and significantly improve the kinetic performance and mechanical stability. Meanwhile, the supported hierarchical microspheres acting as functional cell can provide high active sites, multiple response and suitable environment for immobilizing biomolecules. Different enzymes are immobilized for biosensors. The experiments demonstrate that the effective assembly of hierarchical microspheres into large size ordered architecture by self-supporting branches can significantly enhance the biosensing performance.

*Keywords:* self-assemble, hierarchical structure, hollow, self-supporting, biosensor

* E-mail of corresponding author: huangjy@zju.edu.cn; yezz@zju.edu.cn

## 1. Introduction

Owing to their unique structural features, hierarchical hollow micro-/nanostructures have aroused intense research interest in a wide range of areas such as energy storage and conversion, catalysis, sensors, and biomedical applications [Zhou et al., 2012; Liu et al., 2011; Zhou et al., 2012; Yu et al., 2013; Caruso et al., 1998; Piao et al., 2008; Gao et al., 2007; Zhang et al., 2012; Cao et al., 2013]. Numerous efforts have thus been devoted to develop methods for rational synthesis of hierarchical hollow microspheres, such as, multi-shell, ball in ball type and hollow structures with controlled interior functionalization, which are expected to offer more handles to tailor the properties for different applications [Zhou et al., 2012]. However, the electrode materials are generally fabricated by mixing and stacking, preforming or connecting the isolated microspheres by organic colloid, the intrinsic structure is thus damaged and no well transport channels can be constructed. It causes low kinetic performance and instability, which has become a crucial limitation for further improving the performance. For example, in the applications of biocatalysis and biosensor, previous investigations have shown that the hollow mesoporous microspheres are promising candidates for encapsulating enzymes, due to their large surface area and internal spaces inside the shell, as well as mesoporous environment. However, the major limitation is slow kinetic response and low mechanical stability [Cao et al., 2013; Cao et al., 2011; Vamvakaki et al., 2007; Bulmus et al. 1997]. As for many applications, the disadvantage has become a key restricted factor. Therefore, it has become a crucial challenge to effectively assemble micro-/nanospheres into

large size ordered structures to improve the overall kinetics and mechanical stability [Gur et al., 2006; Wang et al., 2010; Reddy et al., 2009; Ma et al., 2011; Ma et al., 2012; Ma et al., 2013].

In regard to enzymatic biosensor, the enzymes generally catalyze the substrate to cause electrons and mass transfer, however, the intermediate products are usually produced. The second catalysis is thus essential and has become a challenge [Zhou et al., 2005]. Generally speaking, multienzyme and noble metal nanoparticles are introduced to help the second catalysis, however, which causes loss of enzymatic activity, low loading and kinetic response, complex preparation and high cost [Zhai et al. 2013; Huang et al., 2013]. The best condition is the loading matrix itself can afford highly effective second catalysis. As for immobilizing enzymes, it is known that small pores can maintain high loading, low leaching, and improved activities of enzymes, but may cause mass-transfer difficulties and low mechanical stability [Qi et al., 2013; Lee et al., 2005; Zhao et al. 2013]. To overcome these disadvantages, complex hierarchical architectures are desired to be designed to get more handles and achieve improved properties and combined functions. Therefore, hierarchical fabrication at the micro-/nanoscale to integrate multi-functional composite materials has been of great challenge and increasing interest in chemistry, biology and materials science.

Spinel compounds of $AB_2X_4$ (A, B = metal, X = chalcogen) have attracted a great deal of research interest linked to a wide range of applications including electronics and catalysis, magnetism, as well as energy storage and conversion [Sharma et al., 2008; Sharma et al., 2007; Qiu et al., 2010]. Spinel $ZnMn_2O_4$ has been proposed as

one interesting material in view of its low price, abundance and environmental friendliness, multiple valence, prominent Jahn–Teller effect and more importantly the possible synergetic enhancement of the components in such mixed metal oxides [Cheng et al., 2011; Zhao et al., 2013; Zhou et al., 2012; Zhao et al., 2012]. However, it is far more challenging to synthesize and assemble hierarchical hollow microspheres with branches as self-support and transport channels to get improved performance.

Herein, we report the synthesis of $ZnMn_2O_4$ hierarchical hollow microspheres self-supporting architecture (HHMSA) via a facile solvothermal reaction and annealing method. The microspheres are constructed by mesoporous two-layered shell, inner ball and nano-branches to support each other, which provide not only large surface area, ion exchange space, strong mechanical stability, but also 1D integrated transport channels and size matched matrix for functionalization with biomolecules. The fabricated electrodes show significantly enhanced biosensing performance.

## 2. Materials and methods

### 2.1. Synthesis of $ZnMn_2O_4$ HHMSA

A typical synthesis of connected hierarchical $ZnMn_2O_4$ HHMSA was conducted as follows: 0.11 g polyvinyl pyrrolidone (PVP) was firstly dissolved into 50 mL of ethylene glycol (EG) and stirred to form a transparent solution. After this, 0.114 g $Zn(CH_3COO)_2•2H_2O$ and 0.245 g $Mn(CH_3COO)_2•4H_2O$ were then dissolved into the above solution. All the above chemical materials were purchased from Shanghai

Hushi-reagent. The obtained solution was then transferred into a beaker and heated to 170 °C in a drying oven. The solution was kept at 170 °C for 80 min, and then cooled down to 80 °C naturally and taken out. The light brown precipitate was centrifuged at 7000 rpm and washed with ethanol for two times. Then the precipitate was transferred onto Au electrode and dried. Finally, the electrode was annealed at 500 °C in air for 4 h with a slow heating rate of 1 °C $min^{-1}$.

2.2. Characterization of $ZnMn_2O_4$ HHMSA

X-ray diffraction (XRD) patterns were collected on SHIMADZU XRD-6000 Advanced X-Ray Diffractometer with Cu Kα radiation. Field-emission scanning electron microscope (FESEM) images were obtained on a HITACHI SU-70 microscope. Transmission electron microscope (TEM) images were taken on Tecnai G2 F20 S-TWIN, FEI microscopes. The composition of the samples was analyzed by EDX attached to the TEM instrument.

2.3. Fabrication of enzymatic biosensors

The biosensor was prepared as follows: enzymes solution (10.0 mg $ml^{-1}$) was dropped onto the electrode and dried, then the chitosan (CHIT) solution (0.5 wt.%) was further applied onto the electrode surface to further link and prevent possible enzyme leakage. The device was dried at 4 °C overnight in a refrigerator. The electrochemical measurements were carried out on a three-electrode electrochemical workstation (WPG100e electrochemical workstation, Korea) with the modified Au electrode as the working electrode, a saturated calomel electrode (SCE) as a reference electrode, and platinum electrode as a counter electrode.

## 2. Results and discussion

### 3.1. Synthesis and characterization of the $ZnMn_2O_4$ HHMSA

**(the preferred position for Scheme 1)**

The schematic illustration for the fabrication of $ZnMn_2O_4$ HHMSA is shown in Scheme 1. When a certain amount of PVP is dissolved in EG, the micro-emulsion might be formed and acts as the soft template [Wang et al., 2010]. After that, $Zn(CH_3COO)_2•2H_2O$ and $Mn(CH_3COO)_2•4H_2O$ are added into the emulsion and dissolved completely. Due to the strong coordination ability of PVP to metal ions, the $Mn^{2+}$ and $Zn^{2+}$ will be bounded with PVP. During heating, the PVP will aggregate to form a loose ZnMn-glycolate spherical structure in order to reduce the surface energy, but meanwhile some branches are stretched out. When the microspheres are taken out abruptly at proper heating temperature, the branches are preserved and then connect to each other after reducing solvents (see Supporting Information, Fig. S1). After calcinations, the ZnMn-glycolate microspheres shrink and solidify, as a result, the microspheres are self-supported by branches to form an integrated 3D porous architecture. No additional help is needed to build the architecture, so it is a self-assembling process. At the same time, the inner structure of the microsphere also changes. During the heating treatment procedure, a contraction force (Fc) is induced by the oxidative degradation of the organic molecules (such as PVP, EG, $CH_3COOH^-$) [Lai et al., 2011]. Meanwhile, an opposite adhesion force (Fa) is also generated, due to the formation of $ZnMn_2O_4$ crystallites and the release of $CO_2$ gas from the decomposition of organic species [Zhang et al., 2012]. The combined action causes

the separation of the external shell and internal ball. Under the successive action of Fa, the separated shell is further divided into two-layered structure with looser interior and tenser exterior. The XRD pattern (Fig. S2) and EDX spectra (Fig. S3) reveal the pure tetragonal $ZnMn_2O_4$ crystal structure.

**(the preferred position for Fig. 1)**

The morphologies of the prepared $ZnMn_2O_4$ HHMSA are shown in Fig. 1. The whole morphology is a 3D porous architecture, which is constructed by microspheres (500-800 nm) and supporting branches. The fabrication of the 3D porous architecture based electrode is schematically shown in Fig. S4. The microspheres are not simply stacked together, but connected and supported by naturally grown branches (diameter ~ 50 nm, length ~ 100-300 nm) to form some gap. The hierarchical architecture is thus preserved by avoiding aggregating, squashing and destroying. The gap makes reactants easily reach to each microsphere and diffuse randomly, which thus enhances the reactive efficiency. The self-supporting branches act as bridges for electrons and mass transport among each reactive cell (microsphere) that result in timely, fast transport of reactive product, which will further enhance the reactive efficiency. In all, this integrated architecture not only protects the complex structural properties of microspheres for functionalization but also provides enough space and transport network for reactions. The specific structure of the microsphere is shown in Figure 1e. From the broken section, it is observed that the microsphere consists of two parts, the porous inner ball and the separate shell. The inner ball is a solid porous round framework, consisting of connected nanoparticles (diameter ~ 20-40 nm). The shell is

naturally divided into two layers, the looser interior and tenser exterior. Both are constructed by the connected nanoparticles and mesopores. But the nanoparticles in interior have smaller diameter (~ 10 nm) than the exterior (~ 30 nm). There are some advantages of this hierarchical architecture for catalysis and biosensing. First, the mesoporous hollow structure is in favor of reactants adsorption and diffusion, and meanwhile affords hierarchical active sites. Second, the two-layered shell with looser interior and tenser exterior is helpful for enhancing the mechanical stability and preventing the leaching of biomolecules, which is vital for highly efficient immobilization of biomolecules [Vamvakaki et al., 2007; Popat et al., 2011; Zhou et al., 2011; Winkler et al., 2006]. The mesopores in external layer are in favor of attaining high loadings, increasing stability, and protecting the biomolecules from the external environment [Hudson et al., 2008]. Third, the mesoporous inner ball can afford additional active sites to adsorb and clear up the residual substrate that entrances into the hollow sphere, which are favorable to create higher activities and enhance the efficiency.

3.2. Biosensing performance of the prepared biosensors

**(the preferred position for Fig. 2)**

Fig. 2a shows the cyclic voltammetric (CV) behavior of the $ZnMn_2O_4$ HHMSA based electrode in phosphate buffer solution (pH 7.4, 0.10 M). A pair of broadened oxidative and reductive peaks in the potential range of 0.3-1.0 V can be observed, suggesting the oxidation and reduction between Mn species of different states. After adding 2 mM $H_2O_2$, the catalytic oxidation peak current significantly increases to

almost five times of initial current, which reflects the high electrocatalytic activity. The catalytic ability is further revealed by amperometric response (Fig. 2b). The modified electrode responds very rapidly to the addition of $H_2O_2$ and produces steady-state signals within 2 s. The favorable signals are accompanied by a low noise level and long time stability. The catalytic efficiency is much higher than other manganese oxides reported previously [Liu et al., 2005; Li et al., 2010; Yao et al., 2006]. However, when the branches and the microspheres are destroyed and the integrated 3D architecture is broken down (Fig. S5), the response rate and catalytic ability are largely decreased (Fig. 2b insert). After repeated test, we found that the $ZnMn_2O_4$ HHMSA based electrode maintained well stability and repeatability. The results demonstrate that it can significantly enhance the performance by assembling the hierarchical hollow microspheres into self-supporting architecture.

The $ZnMn_2O_4$ HHMSA is further used to immobilize biomolecules for biosensing. Choline oxidase (ChOx) is first employed for choline detection. It is observed that the addition of choline causes significantly increase of oxidation current (Fig. S6). The response time is less than 2 s (Fig. 2c), which is much faster than other manganese oxides nanomaterials without wiring [Claudio et al., 2013; Bai et al., 2007; Dontsova et al., 2011; Bai et al., 2008]. The equal addition of substrate causes a stepped responding curve that increases with the concentration (Fig. 2c, d). The biosensor exhibits high sensitivity (124.4 μA $mM^{-1}$ $cm^{-2}$), wide linear range ($1\times10^{-6}$ ~ $1.2\times10^{-3}$ M), and low detection limit (1 μM, S/N = 3). The stability is measured by monitoring the response on successively cycling the electrode, it is found that the response shows

negligible change after 20 cycles. Compared with other electrode materials, the HHMSA has much better performance in response time, sensitivity and stability (Table S1). However, the linear range and limit of detection of prepared biosensor is not so well comparing with some other methods (Table S1). The high performance can be attributed to following facts: (i) the widely distributed mesopores provide scale-adaptive cells for holding enzymes and friendly microenvironment for retaining their intrinsic structure that is vital to retain enzymatic activity, (ii) the hierarchical hollow structure provides enough active sites and multiple response mechanism (Fig. 3e), (iii) the supporting branches provide electrons and mass transport channels to achieve high kinetic performance, (iv) the two-layered shell enhances the mechanical stability of the microspheres and the integrated 3D framework strengthens the soundness of the architecture and prevents squashing and destroying. The advantages are further confirmed by immobilizing glucose oxidase (GOx) for glucose biosensing (Fig. S7).

## 3. Conclusions

In summary, we demonstrated a facile and scalable approach to fabricate and self-assemble the hierarchical hollow microspheres into self-supporting architecture by naturally grown branches. The hierarchical architecture can provide high active sites, multiple response, mesoporous/macroporous environment, integrated transport channels, improved kinetic response and high stability. The prepared biosensors show significantly improved biosensing performance. This self-supporting architecture

opens a way to effectively apply micro-/nanospheres as high performance electrode materials for biosensing.

**Acknowledgments**

This work was financially supported by National Natural Science Foundation of China (91333203), the Doctorate Fund of the Ministry of Education under grant no. 2011010110013 and the Innovation team of Zhejiang province No. 2010R50020.

**References**

Bai Y.H., Du Y., Xu J.J., Chen H.Y., 2007. Electrochem. Comm. 9, 2611-2616.

Bai Y.H., Zhang H., Xu J.J., Chen H.Y., 2008. J. Phys. Chem. C, 112, 18984-18990.

Bulmus V., Ayhan H., Piskin E., 1997. Chem. Eng. J. 65, 71-76.

Gao J., Liang G., Zhang B., Kuang Y., Zhang X., Xu B., 2007. J. Am. Chem. Soc. 129, 1428-1433.

Cao S., Fang L., Zhao Z., Ge Y., Piletsky S., Turner A. P. F., 2013. Adv. Funct. Mater. 23, 2162-2167.

Cao S., Zhao Z., Jin X., Sheng W., Li S., Ge Y., Dong M., Wu W., Fang L., 2011. J. Mater. Chem. 21, 19124-19131.

Caruso F., Caruso R.A., Mohwald H., 1998. Science, 282, 1111-1114.

Cheng F., Shen J., Peng B., Pan Y., Tao Z., Chen J., 2011. Nature Chem. **3**, 79-84.

Claudio M., Massimo C., Antonietta T., Benedetto B., 2013. Electrochim. Acta, 87, 918-924.

Dontsova E.A., Zeifman Y.S., Budashov I.A., Eremenko A.V., Kalnov S.L., Kurochkin I.N., 2011. Sens. Actuators B Chem. 159, 261-270.

Gur L., Fromer N.A., Chen C.P., Kanaras A.G., Alivisatos A.P., 2006. Nano. Lett. **7**, 409-414.

Huang X., Wang J., Liu H., Lan T., Ren J., 2013. Talanta, **106**., 79-84.

Hudson S., Magner E., Cooney J., 2008. Angew. Chem. Int. Ed., 47, 8582.

Lai X.Y., Li J., Korgel B.A., Dong Z.H., Li Z.M., Su F.B., Du J.A., Wang D., 2011. Angew. Chem. Int. Ed. 50, 2738-2741.

Lee D., Lee J., Kim J., Na H.B., Kim B., Shin C.H., Kwak J.H., Dohnalkova A., Grate J.W., Hyeon T., Kim H.S., 2005. Adv. Mater., 17, 2828-2833.

Li L., Du Z., Liu S., Hao Q., Wang Y., Li Q., Wang T., 2010. Talanta, 82, 1637-1641.

Lin Y., Cui X., Li L., 2005. Electrochem. Commun. **7**, 166-172.

Liu J., Zhou Y.C., Wang J.B., Pan Y., Xue D., 2011. Chem. Commun. 47, 10380-10382.

Ma Y., Fang C., Ding B., Ji G., Lee J.Y., 2013. Adv. Mater., 25, 4646-4652.

Ma Y., Ji G., Lee J.Y., 2011. J. Mater. Chem., 21, 13009-13014.

Ma Y., Ji G., Ding B., Lee J.Y., 2012. J. Mater. Chem. 22, 24380-24385.

Piao Y., Kim J., Bin Na H., Kim D., Baek J.S., Ko M.K., Lee J.H., Shokouhimehr M., Hyeon T., 2008. Nature Mater. **7**, 242-247.

Popat A., Hartono S.B., Stahr F., Liu J., Qiao S., Lu G., 2011. Nanoscale, 3, 2801-2818.

Qi Z., Weissmuller J., 2013. ACS Nano, **7**, 5948-5954.

Qiu Y.C., Yang S.H., Deng H., Jin L.M., Li W.S., 2010. J. Mater. Chem. 20, 4439-4444.

Reddy A.L.M., Shaijumon M.M., Gowda S.R., Ajayan P.M., 2009. Nano. Lett. 9, 1002-1006.

Sharma Y., Sharma N., Rao G.V.S., Chowdari B.V.R., 2008. Electrochim. Acta, 53, 2380-2385.

Sharma Y., Sharma N., Rao G.V.S., Chowdari B.V.R., 2007. Adv. Funct. Mater. 17, 2855-2861.

Sharma Y., Sharma N., Rao G. V.S., Chowdari B.V.R., 2007. J. Power Sources, 173, 495-501.

Vamvakaki V., Chaniotakis N. A., 2007. Biosens. Bioelectron. 22, 2650-2655.

Wang H., Cui L.F., Yang Y., Sanchez Casalongue H., Robinson J.T., Liang Y., Cui Y., Dai H., 2010. J. Am. Chem. Soc., 132, 13978-13980.

Wang X., Wu X.L., Guo Y.G., Zhong Y.T., Cao X.Q., Ma Y., Yao J.N., 2010. Adv. Funct. Mater. 20, 1680-1686.

Winkler R., Richter M.E.A., Knupfer U., Merten D., Hertweck C., 2006. Angew. Chem. Int. Ed. 45, 8016-8018.

Yao S., Xu J., Wang Y., Chen X., Xu Y., Hu S., 2006. Anal. Chim. Acta, 557, 78-84.

Yu L., Wu H.B., Lou X.W., 2013. Adv. Mater. 25, 2296-2300.

Zhai D., Liu B., Shi Y., Pan L., Wang Y., Li W., Zhang R., Yu G., 2013. ACS Nano, **7**, 3540-3546.

Zhang G., Yu L., Wu H.B., Hoster H.E., Lou X.W., 2012. Adv. Mater. 24, 4609-4613.

Zhao J., Wang F., Su P., Li M., Chen J., Yang Q., Li C., 2012. J. Mater. Chem. 22, 13328-13333.

Zhao L., Li X., Zhao J., 2013. Appl. Surf. Sci. 268, 274-277.

Zhao M., Huang J., Zhou Y., Pan X., He H., Ye Z., Pan X., 2013. Chem. Commun. 49, 7656-7658.

Zhao M., Huang J., Zhou Y., Chen Q., Pan X., He H., Ye Z., 2013. Biosens. Bioelectron., 43, 226-230.

Zhao M., Li Z., Han Z., Wang K., Zhou Y., Huang J., Ye Z., 2013. Biosens. Bioelectron. 49, 318-322.

Zhou H., Chen H., Luo S., Chen J., Wei W., Kuang Y., 2005. Biosens. Bioelectron., 20, 1305-1311.

Zhou L., Wu H.B., Zhu T., Lou X.W., 2012. J. Mater. Chem. 22, 827-829.

Zhou L., Zhao D., Lou X.W., 2012. Adv. Mater. 24, 745-748.

Zhou L., Zhao D.Y., Lou X.W., 2012. Angew. Chem. Int. Ed. 51, 239-241.

Zhou Z., Taylor R.N.K., Kullmann S., Bao H., Hartmann M., 2011. Adv. Mater. 23, 2627-2632.

**Captions**

**Scheme 1.** Schematic diagram: (a) the formation of hierarchical $ZnMn_2O_4$ hollow microspheres with branches and (b) the self-assembly process of the microspheres to form an integrated 3D architecture.

**Fig. 1.** SEM images (a-c) and schematic diagram of the self-supporting $ZnMn_2O_4$ microspheres. SEM images of the surface (d) and broken structure (e) of the microspheres. Schematic diagram (f) of the hierarchical structure.

**Fig. 2.** CV curves (a) of the $ZnMn_2O_4$ HHMSA based electrode in absence and presence of $H_2O_2$. The amperometric response curves of the electrode fabricated by the $ZnMn_2O_4$ HHMSA (b) and the damaged $ZnMn_2O_4$ microspheres without branches to connect each other (b insert). Typical current–time response curve (c) of the prepared choline biosensor for successive addition of choline with a step of 0.1 mM under stirring. The calibration curve (d) of the choline concentration versus current. Schematic illustration (e) of the advantages of the $ZnMn_2O_4$ HHMSA for multiple responses, immobilizing enzymes and transporting electrons.

The hierarchical hollow microspheres are assembled to self-supporting architecture.

The branches can afford transport channels and improve the kinetic performance.

The hierarchical microspheres act as functional cell for immobilizing biomolecule.

Assembling microspheres to ordered architecture enhances the biosensing performance.

This architecture can be used for fabricating high performance biosensors.

Fig 1

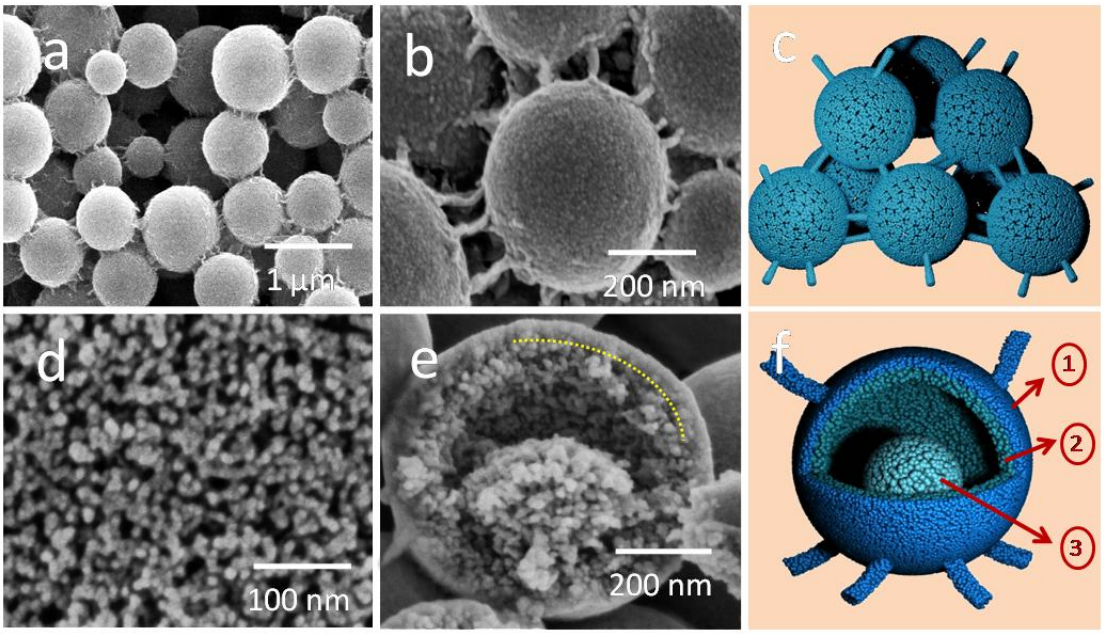

Fig 2

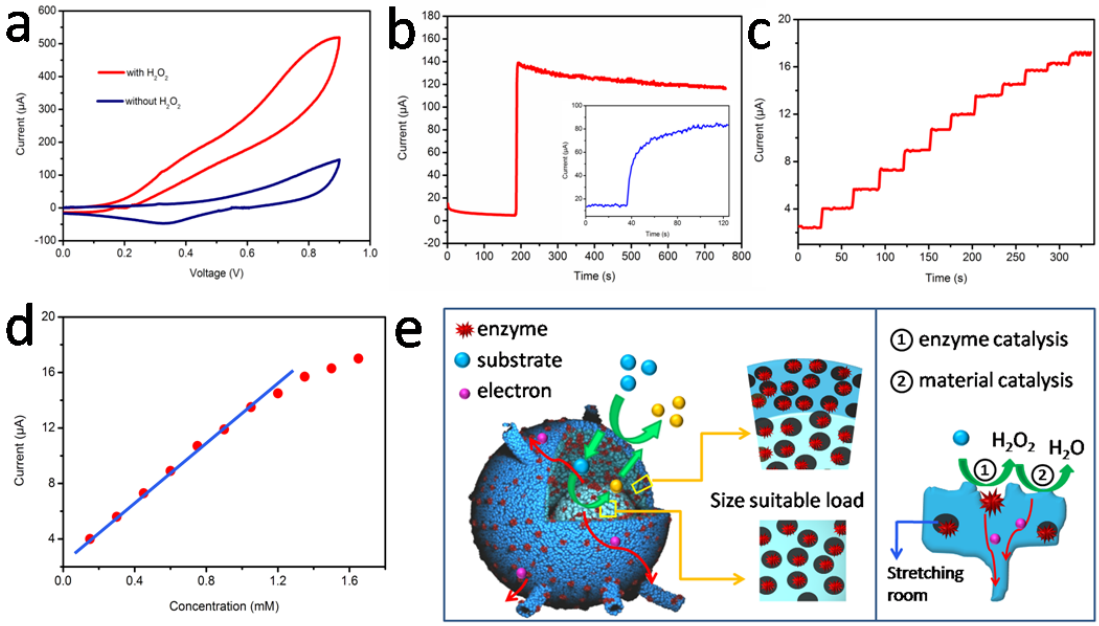

**Scheme 1**